International Journal of Computer Mathematics
Vol. 83, No. 1, January 2006, 49–57

Taylor & Francis
Taylor & Francis Group

Intensity-based robust similarity for multimodal image registration

JUAN DU†‡, SONGYUAN TANG†§, TIANZI JIANG*† and ZHENSU LU‡

†National Laboratory of Pattern Recognition, Institute of Automation, Chinese Academy of Sciences, Beijing 100080, P. R. China
‡School of Information Science and Engineering, Lanzhou University, Lanzhou 730000, P. R. China
§Opto-electronic Engineering, Beijing Institute of Technology, Beijing 100081, P. R. China

(Received 10 January 2005)

This paper proposes a new intensity-based similarity metric that can be used for the registration of multimodal images. It combines the robust estimation with both the forward and inverse transformation to reduce the negative effects of outliers in the images. For this purpose, we firstly employ the multiresolution technique to downsample the original images, then resort to the simulated annealing method to initialize the transformation parameters at the coarsest resolution. Finally the Powell method is utilized to obtain the optimal transformation parameters at each resolution. In our experiments, the new method is compared to other popular similarity measures, on the synthetic data as well as the real data, and the experimental results are encouraging.

Keywords: Multimodal registration; Forward and inverse transform; Robust estimation; Multiresolution technique; Optimization

C.R. Category: I.4.3

1. Introduction

Medical images provide information about pathology and associated anatomy of the human body. Clinicians often wish to compare two or more images of the same anatomical regions acquired under different modalities since these images can provide complementary information. For example, position emission tomography (PET) provides information about a specific function such as cerebral blood flow or the density of receptor in a certain area, and magnetic resonance imaging (MRI) provides information about morphology and the topology of structures. Once PET and MRI have been matched well, clinicians can easily estimate the place of pathological changes. However, it is impractical for a clinician to align many images manually. Therefore it is highly desirable to develop methods for dealing with this issue. Medical image registration aims at solving such problems.

*Corresponding author. Email: jiangtz@nlpr.ia.ac.cn

International Journal of Computer Mathematics
ISSN 0020-7160 print/ISSN 1029-0265 online
http://www.tandf.co.uk/journals
DOI: 10.1080/00207160500112944

Over the past two decades, many techniques have been proposed for image registration. In general, they are classified as the feature based [1–6] or intensity based [7–15]. Feature-based techniques extract the features of anatomical structures from volume data such as landmarks, surfaces or contours, and attempts to find the correspondence between them. The matching result is critically dependent on the quality of the feature extraction. Since the anatomical structures have complex shapes, human interaction is often needed to help select or extract the features which is inconvenient. Intensity-based techniques operate on the image intensity value directly and can be performed automatically. They are widely employed in the multimodal image registration. Popular algorithms include the partitioned intensity uniformity technique (PIU) [9], which minimizes the variance of intensity ratios, and the mutual information technique (MI), which maximizes mutual information [10–15]. These methods can give better results.

If images are corrupted by outliers or non-Gaussian noises, registration becomes difficult. Usually, the results using different direction transformation are different. In this paper, we propose a novel intensity-based similarity technique to match multimodal brain images. A robust estimator is used to reduce the effect of outliers or noise and to make the cost function smooth. Both forward and inverse transforms are employed by the similarity metric to increase the accuracy in the registration. The Powell method and the multiresolution technique are introduced to optimize the transform parameters. To obtain a better initial point, a simulated annealing method is employed. Since simulated annealing is slow, we only use it at the coarsest resolution.

The paper is organized as following. In section 2, we briefly present two popular standard similarity metrics, PIU and MI. In section 3, we describe on our new method. Then in section 4, we compare the proposed method with PIU and MI, using both synthetic and real data. Section 5 contains the conclusions.

2. Standard similarity measures

2.1 *Partitioned intensity uniformity (PIU) method*

The intensity-based method used for multimodality registration was proposed by Woods *et al.* [9] based on the idealized assumption that a uniform region in one image corresponds to a region that is also uniform in the other image. The voxels in the uniform region should have the same intensity value and represent the same tissue. Thus a target image is partitioned into an isointensity set, usually 256 bins. The partitioned regions represent the spatial information and are mapped to the float image. The process produces the same two segmented images. When the images are aligned, the expected values μ_i and the standard deviations σ_i of the segmented regions of the float image are computed. If the two images match correctly, the ratio of the normalized standard deviation σ_i to the expected value μ_i in each region should be minimal. The PIU method calculates the weighted average of the ratio in all regions:

$$\mathrm{PIU} = \sum_{i=0}^{255} \frac{n_i}{N} \frac{\sigma_i}{\mu_i} \tag{1}$$

where

$$\mu_i = \frac{1}{n_i} \sum_{\vec{x} | I_{\mathrm{target}}(\vec{x}) = i} [I_{\mathrm{float}}(T(\vec{x}))] \quad i = 0, 1, \ldots, 255 \tag{2}$$

$$\sigma_i = \frac{1}{n_i - 1} \sum_{\vec{x}|I_{\text{target}}(\vec{x})=i} [I_{\text{float}}(T(\vec{x})) - \mu_i]^2 \quad i = 0, 1, \ldots, 255 \tag{3}$$

where n_i is the number of ith partitioned regions of the target image with intensity value i and N is the total number of voxels in the images. The value of PIU determines the matching result: the lower PIU, the more accurately the images match. When the method is used for PET–MRI registration, the scalp in the MRI is required to be moved first so that uniformity is satisfied.

However, the uniformity assumption may only define a crude approximation in some cases [9]. In particular, when the effect of outliers in images is not taken into consideration, the registration accuracy will be affected. Robust estimator and double-directional transformation can cope efficiently with this problem. In the following section, we apply them to the cost function (1), and as shown in section 4, the results show better accuracy than PIU.

2.2 *Mutual information (MI) method*

The MI method [11] applies mutual information $\mathrm{I}(I_{\text{target}}(\cdot), I_{\text{float}}(T(\cdot)))$ to image registration, which is assumed to be maximal if the images are correctly aligned. The cost function can be expressed as

$$\mathrm{I}(I_{\text{target}}(\cdot), I_{\text{float}}(T(\cdot))) = \sum_{i=0}^{I-1} \sum_{j=0}^{J-1} p(i, j) \log \frac{p(i, j)}{p(i)p(j)} \tag{4}$$

where I and J are the number of grey levels of I_{target} and I_{float}. The joint probabilities $p(i, j)$ are the elements of the co-occurrence matrix of $I_{\text{target}}(\cdot)$ and $I_{\text{float}}(T(\cdot))$, and $p(i)$ and $p(j)$ are the marginal probabilities of $I_{\text{target}}(\cdot)$ and $I_{\text{float}}(T(\cdot))$, respectively. This method is quite good for multimodal situations. We will compare it with our new method in section 4.

3. Proposed method

3.1 *Similarity metric*

When two images are registered, it is difficult to satisfy the uniformity hypothesis completely if there are outliers of non-Gaussian noise distribution in the images. When there are many outliers, the result of registration is affected negatively because they have such a strong effect on the minimization that the parameter estimation is distorted. To obtain a better registration result, the negative effect of outliers or non-Gaussian noises should be counteracted. Robust estimators [17] are widely adopted to solve such problems. The M-estimator is a type of robust estimator which has been utilized as a useful tool in image processing [16, 18, 19]. The robust function increases more slowly than the quadratic function. In fact, M-estimators give the outliers or noise the less weight. In this paper, we use Tukey's bi-weight estimator [20] which is described by the following equation:

$$\rho(x) = \begin{cases} c^2/6\{1 - [1 - (x/c)^2]^3\} & \text{if } |x| \le c \\ c^2/6 & \text{if } |x| > c \end{cases} \tag{5}$$

$$\varphi(x) = \begin{cases} x[1 - (x/c)^2]^2 & \text{if } |x| \le c \\ 0 & \text{if } |x| > c \end{cases} \tag{6}$$

$$\omega(x) = \begin{cases} [1 - (x/c)^2] & \text{if } |x| \le c \\ 0 & \text{if } |x| > c \end{cases} \tag{7}$$

where $\rho(x)$ is the robust estimator function, and $\varphi(x)$ and $\omega(x)$ are its influence function and its weight function (figure 1).

In the PIU method, both the target image and the float image are partitioned and the segmented regions are projected on the target image. However, the matching results are inconsistent. For two images overlapping at some position, we can transform the float image or inversely transform the target image. In the proposed method, to improve the registration accuracy, both images are partitioned and the partitioned regions are mapped to each other. By adopting the forward and inverse transform, we define a similarity metric DRPIU (double directional PIU) as follows:

$$\text{DRPIU} = \sum_{i=0}^{255} \frac{n_i}{N} \frac{\sigma_i}{\mu_i} + \lambda \sum_{j=0}^{255} \frac{n_j}{N} \frac{\sigma_j}{\mu_j} \tag{8}$$

where

$$\mu_i = \frac{1}{n_i} \sum_{\vec{x}|I_{\text{target}}(\vec{x})=i} [I_{\text{float}}(T(\vec{x}))] \quad i = 0, 1, \ldots, 255 \tag{9}$$

$$\sigma_i = \frac{1}{n_i - 1} \sum_{\vec{x}|I_{\text{target}}(\vec{x})=i} [\rho_1(I_{\text{float}}(T(\vec{x}) - \mu_i))]^2 \quad i = 0, 1, \ldots, 255 \tag{10}$$

$$\mu_j = \frac{1}{n_j} \sum_{\vec{x}|I_{\text{float}}(\vec{x})=j} [I_{\text{target}}(T^{-1}(\vec{x}))] \quad j = 0, 1, \ldots, 255 \tag{11}$$

$$\sigma_j = \frac{1}{n_j - 1} \sum_{\vec{x}|I_{\text{target}}(\vec{x})=j} [\rho_2(I_{\text{target}}(T^{-1}(\vec{x}) - \mu_j))]^2 \quad j = 0, 1, \ldots, 255. \tag{12}$$

In equation (8), λ is a weighted parameter which ensures that both direction matching results are consistent. In equation (5), $\rho_1(\cdot)$ and $\rho_2(\cdot)$ are different estimator functions with different values of C. The values of λ and C depend on experiment.

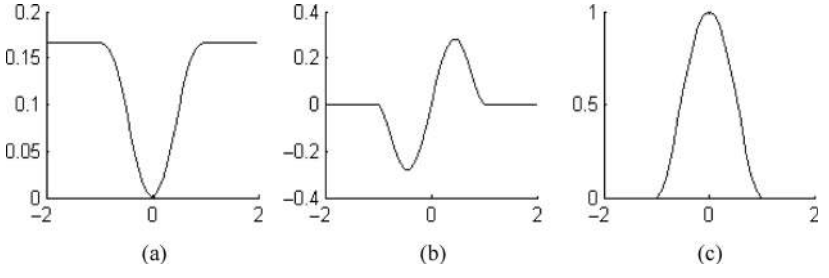

Figure 1. (a) The robust estimator function $\rho(x)$, (b) the influence function $\varphi(x)$ and (c) the weight function $\omega(x)$ for $c = 1$.

3.2 *Transformation*

In the present study, we only consider the rigid three-dimensional transformation $T_{\text{rigid}}(\vec{x})$, which first rotates an image and then translates it. The transformation can be represented as

$$T_{\text{rigid}}(\vec{x}) = \begin{pmatrix} \cos\beta\cos\gamma & \cos\alpha\sin\gamma + \sin\alpha\sin\beta\cos\gamma & \sin\alpha\sin\gamma - \cos\alpha\sin\beta\cos\gamma & t_x \\ -\cos\beta\sin\gamma & \cos\alpha\cos\gamma - \sin\alpha\sin\beta\sin\gamma & \sin\alpha\cos\gamma + \cos\alpha\sin\beta\sin\gamma & t_y \\ \sin\beta & -\sin\alpha\cos\beta & \cos\alpha\cos\beta & t_z \\ 0 & 0 & 0 & 1 \end{pmatrix} \tag{13}$$

where α, β and γ are the rotations around the x, y and z axes, respectively, and t_x, t_y and t_z are the displacements on the x, y and z axes, respectively.

When one volume is transformed, its grid points do not usually coincide exactly with the grid points of another volume. To obtain the voxel pairs for the calculation, interpolation is required. There are many interpolation methods, such as nearest-neighbour interpolation, trilinear interpolation or sinus cardinal interpolation. The nearest-neighbour interpolation is fast but does not achieve a high degree of accuracy. The sinus cardinal interpolation gives the best results but has a high computational cost. Therefore, as a compromise, we adopted the trilinear interpolation in this study.

3.3 *Optimization*

The conventional optimization method, the Powell search [21], is used to obtain the transformed parameters. In this method it is not necessary to calculate derivatives of the cost function. It is a robust direction search method in which the direction of the search space is repeatedly iterated. A set of directions are defined and a search is performed in one direction until a minimum is found; a second search is then perfomed from this minimum in the next direction until another minimum is found, and so on. After all the directions have been searched, the direction is updated and the one-dimensional search method is repeated until convergence is reached. This method cannot guarantee finding the global optimal value as it is easily trapped in local minima. The global optimal result can only be found effectively when the initial point is near the global optimal value. To solve this problem, we adopt global optimization simulated annealing [22] to determine the initial point. If we apply simulated annealing to the original data, it will be very slow. Thereby we use a multiresolution approach, which not only improves the speed of the optimization, but also effectively avoids local minima. The images are equidistantly subsampled by a factor 2 in each dimension. The optimization procedure is from coarse to fine. The simulated annealing method is only used at the coarsest resolution images and selects a large stochastic search step to speed the convergence. This technique guarantees that the initial point will be near the global optimum and the speed of execution is not affected.

4. Experimental results

Synthetic MRI images T1 and T2 obtained from the Brainweb Database [23] were used to evaluate our method. The images are different modalities and are correctly registered. The image size is $181 \times 217 \times 181$ and the voxel size is $1\,\text{mm} \times 1\,\text{mm} \times 1\,\text{mm}$. The image slices are shown in figure 2. Outliers were simulated by adding the 10% salt-and-pepper noise

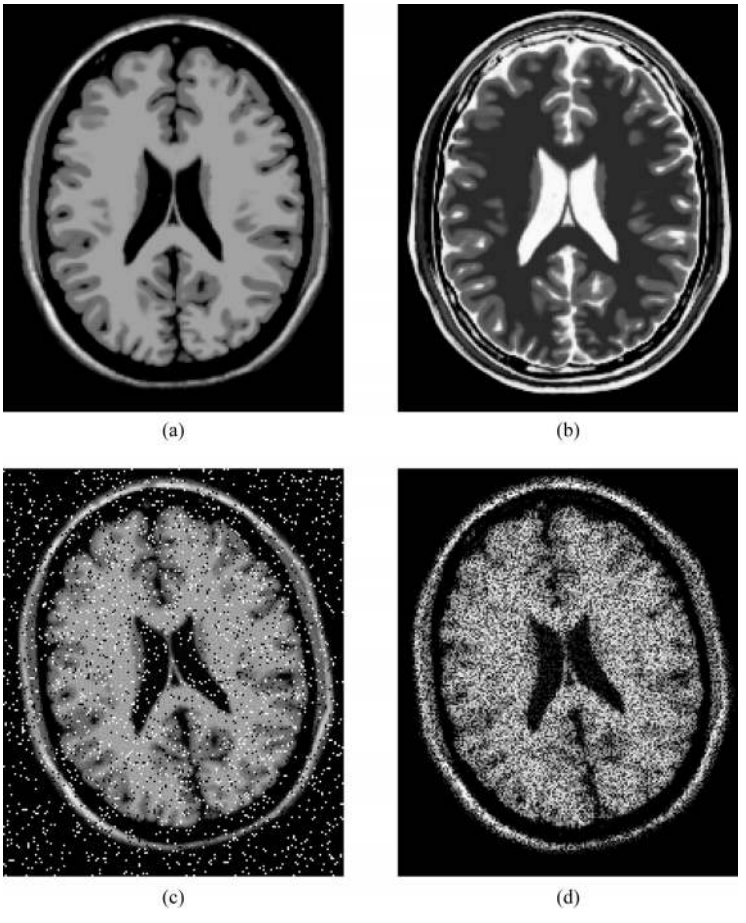

Figure 2. Image slices: (a) mr_T1 image; (b) mr_T2 image; (c) image (a) rotated by $-10°$ along the z axis, translated by 10 voxels along the x axis and by -10 pixels along the y axis, with 10% salt-and-pepper noise added; (d) image (a) rotated by $-10°$ along the z axis, translated by 10 voxels along the x axis and -10 pixels along the y axis, and with 10% speckle noise added.

Table 1. The expected value and the standard deviation of the registration error on the transform parameters computed on a set of 20 different registration problems which were artificially predetermined transformations to mr_T1 involving translation parameters between -15 and 15 voxels and rotations between $-15°$ and 15° with the addition of 10% salt-and-pepper noise.

Method	$\Delta\theta_x$ (deg)	$\Delta\theta_y$ (deg)	$\Delta\theta_z$ (deg)	Δt_x (mm)	Δt_y (mm)	Δt_z (mm)
PIU	0.21 ± 0.19	0.24 ± 0.17	0.29 ± 0.34	0.76 ± 0.60	0.37 ± 0.32	0.65 ± 0.49
MI	0.05 ± 0.03	0.10 ± 0.11	0.16 ± 0.15	0.22 ± 0.30	0.20 ± 0.25	0.20 ± 0.24
DRPIU	0.07 ± 0.03	0.13 ± 0.12	0.08 ± 0.07	0.21 ± 0.27	0.18 ± 0.10	0.16 ± 0.13

Table 2. The expected value and the standard deviation of the registration error on the transform parameters computed on a set of 20 different registration problems which were artificially predetermined transformations to mr_T1 involving translation parameters between -15 and 15 voxels and rotations between $-15°$ and 15° with the addition of 10% speckle noise.

Method	$\Delta\theta_x$ (deg)	$\Delta\theta_y$ (deg)	$\Delta\theta_z$ (deg)	Δt_x (mm)	Δt_y (mm)	Δt_z (mm)
PIU	0.08 ± 0.07	0.25 ± 0.32	0.33 ± 0.30	1.25 ± 1.69	0.50 ± 0.43	0.36 ± 0.46
MI	0.40 ± 0.56	1.00 ± 1.13	0.51 ± 0.18	1.10 ± 0.85	0.90 ± 0.36	1.13 ± 1.02
DRPIU	0.10 ± 0.05	0.10 ± 0.05	0.08 ± 0.06	0.05 ± 0.04	0.09 ± 0.06	0.12 ± 0.06

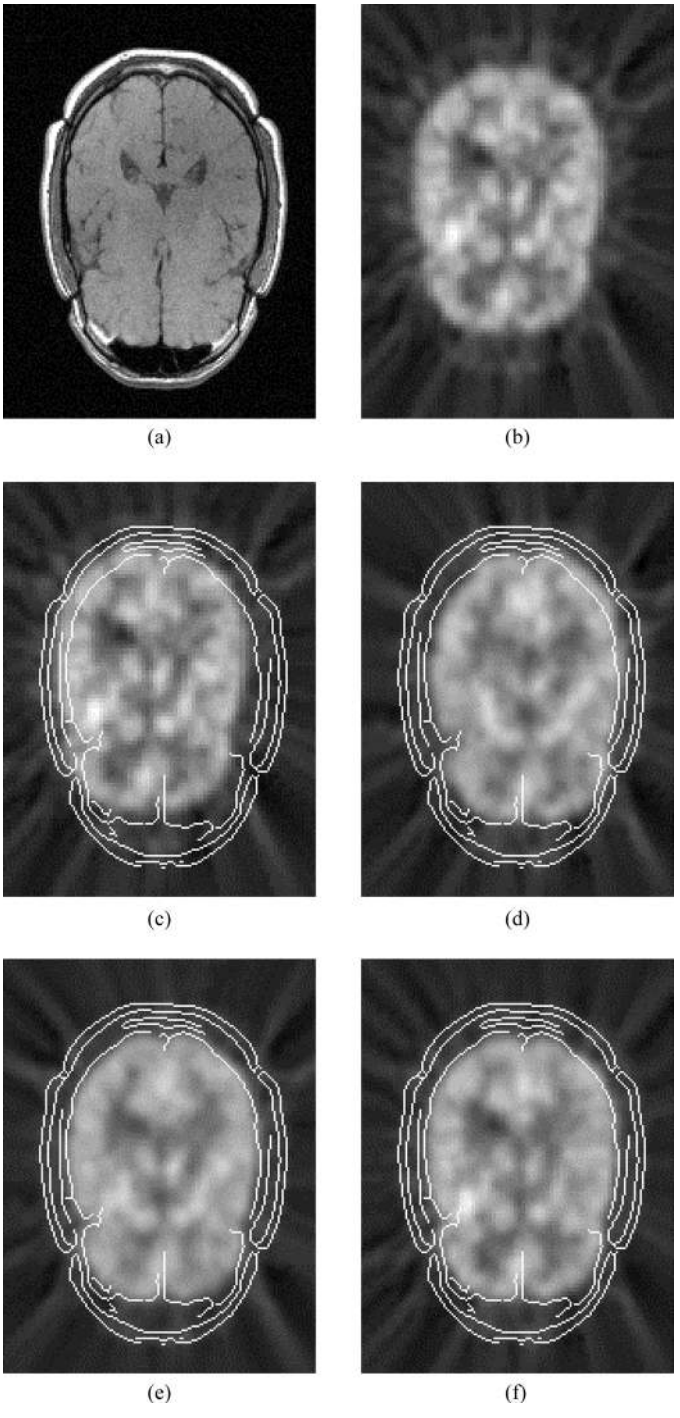

Figure 3. MRI–PET scan registration of the brain of the same patient: (a) MRI image; (b) PET image; (c) contour of the MRI image superimposed on the PET image before registration; (d) contour of the MRI image superimposed on the PET image using the PIU method after registration (non-brain regions have not been removed); (e) contour of the MRI image superimposed on the PET image using the MI method after registration; (f) contour of the MRI image superimposed on the PET image using the proposed DRPIU method after registration.

or 10% speckle noise to the T1 volumes. The expected value and the standard deviation of the registration error on the transform parameters were computed on a set of 20 different registration problems, which were artificially predetermined transformations to T1 involving translation parameters between -15 and 15 voxels and rotations between $-15°$ and $15°$. Examples are shown in figures 2(c) and 2(d).

The proposed method was compared with the MI and PIU techniques, and the results are shown in tables 1 and 2. Table 1 shows the results obtained for T1 images with salt-and-pepper noise. The results of the proposed method and the MI method have the same accuracy and are significantly better than those of PIU. Table 2 shows the results obtained for T1 images with speckle noise, and in this case the proposed method gives the best registration accuracy.

The computation and optimization processes used in each method were performed on a Pentium III PC equipped with 512 RAM. The execution times were as follows: PIU method, about 15 min; MI method, about 19 min; our proposed method, about 29 min.

We also used actual patient data to test our method. We used a patient's brain PET scan registered to its MRI scan; their sizes are $256 \times 256 \times 26$ and $128 \times 128 \times 15$ and their voxel sizes are $1.25\,\text{mm} \times 1.25\,\text{mm} \times 4\,\text{mm}$ and $2.6\,\text{mm} \times 2.6\,\text{mm} \times 8\,\text{mm}$, respectively [figures 3(a) and 3(b)]. The non-brain regions were not removed from the MRI scan and were considered as outliers. Figure 3(c) shows the contour of the MRI scan superimposed on the PET scan before registration. Figures 3(d), 3(e) and 3(f) show the results of the PIU, MI and the proposed DRPIU methods, respectively. It can easily be seen that both MI and the proposed method give good results. In addition, the accuracy of our method has been considered satisfactory by an expert.

5. Conclusion

We have developed a novel intensity-based similarity measure for multimodal images. We have employed the robust estimator to reduce the negative affect of outliers or non-Gaussian noise. Both forward and inverse transformation is used to improve the accuracy of the registration results. To avoid the local minima, global optimization–simulated annealing was applied. However, the optimization speed is very slow if applied to the original data, and so we combined the multiresolution technique and the Powell method. The simulated annealing method was only used at the coarsest resolution images to guarantee that the initial point was near the global optimum.

We have compared our new method with the commonly used PIU method and the MI method. The results show that our method is more accurate although it requires more computation time. It can be used to improve accuracy in a number of critical image registration problems.

Acknowledgements

This work was partially supported by the Hundred Talents Program of the Chinese Academy of Sciences, the Natural Science Foundation of China (Grants 30425004 and 60121302) and the State Commission of Science and Technology of China (Grant 2003CB716104).

References

[1] Fitzpatrick, J., West, J. and Maurer, C., Jr., 1998, Predicting error in rigid-body, point-based registration. *IEEE Transactions on Medical Imaging*, **17**, 694–702.

[2] Frantz, S., Rohr, K., Stiehl, H.S., Kim, S.-I. and Weese, J., 1999, Validating point-based MR/CT registration based on semi-automatic landmark extraction. *Proceedings of CARS'99* (Asterdam: Elsevier Science), pp. 233–237.
[3] Lemoine, D., Liegeard, D., Lussot, D. and Barillot, C., 1994, *Proceedings of SPIE*, **2164**, 46–56.
[4] Davatzikos, C., Prince, J.L. and Bfyan, R.N., 1996, Image registration based on boundary mapping. *IEEE Transactions on Medical Imaging*, **15**, 112–115.
[5] Hsu, L., Loew, M.H. and Ostuni, L.J., 1999, Automated registration of CT and MR brain images using hierarchical shape representation. *IEEE Engineering in Medicine and Biology Magazine*, **18**, 40–47.
[6] Besl, P.J. and McKay, N.D., 1992, A method for registration of 3-D shapes. *IEEE Transactions on Pattern Analysis and Machine Intelligence*, **14**, 239–256.
[7] Banerjee, P.K. and Toga, A.W., 1994, Image alignment by integrated rotational and translational transformation matrix. *Physics in Medicine and Biology*, **39**, 1969–1988.
[8] Hajnal, J.V., Saeed, N., Oatridge, A., Williams, E.J., Young, I.R. and Bydder, G.M., 1995, Detection of subtle brain changes using subvoxel registration and subtraction of serial MR images. *Journal of Computer Assisted Tomography*, **19**, 667–691.
[9] Woods, R.P., Mazziotta, J.C. and Cherry, S.R., 1993, MRI-PET registration with automated algorithm. *Journal of Computer Assisted Tomography*, **17**, 536–546.
[10] Maes, F., Collignon, A., Vandermeulen, D., Marchal, G. and Suetens, P., 1997, Multimodality image registration by maximization of mutual information. *IEEE Transactions on Medical Imaging*, **16**, 187–198.
[11] Thevenaz, P. and Unser, M., 2000, Optimization of mutual information for multiresolution image registration. *IEEE Transactions on Image Processing*, **9**, 2083–2099.
[12] Ding, E., Kularatna, T., Goshtasby, A. and Satter, M., 2000, Volumetric image registration by template matching. In: *Medical Imaging 2000* (Bellingham, WA: SPIE), pp. 1235–1246.
[13] Studholme, C., Hill, D.E.G. and Hawkes, D.J., 1996, Automated 3D registration of MR and CT images of the head. *Medical Image Analysis*, **1**, 163–175.
[14] Shekhar, R. and Zagrodsky, V., 2002, Mutual information-based rigid and nonrigid registration of ultrasound volumes. *IEEE Transactions on Medical Imaging*, **21**, 9–22.
[15] He, R. and Narayana, P.A., 2002, Global optimization of mutual information: application to three-dimensional retrospective registration of magnetic resonance images. *Computerized Medical Imaging and Graphics*, **26**, 277–292.
[16] Hellier, P., Barillot, C., Memin, E. and Perez, P., 2001, Hierarchical estimation of a dense deformation field for 3-D robust registration. *IEEE Transactions on Medical Imaging*, **20**, 388–402.
[17] Meer, P., Mintz, D., Rosenfeld, A. and Kim, D.Y., 1990, Robust regression method for computer vision: a review. *International Journal of Computer Vision*, **6**, 59–70.
[18] Nikou, C., Heitz, F., Armspach, J.P., Namer, I.J. and Grucker, D., 1998, MR/MR and MR/SPECT registration of brain images using robust voxel similarity metrics. *NeuroImage*, **8**, 30–43.
[19] Black, M.J. and Rangarajan, A., 1996, On the unification of line processes, outliers rejection and robust statics in early vision. *International Journal of Computer Vision*, **19**, 57–91.
[20] Huber, P.J., 1981, *Robust Statistics* (New York: Wiley).
[21] Press, W.H., Flannery, B.P., Teukolsky, S.A. and Vetterling, W.T., 1992, *Numerical Recipes in C* (Cambridge: Cambridge University Press).
[22] Ingber, L., 1995, Adaptive simulated annealing (ASA). Technical Report, Lester Ingber Research, McLean, VA.
[23] Cocosco C.A., Kollokian, V., Kwan, R.K.-S. and Evans, A.C., 1997, Brain web: online interface to a 3D MRI simulated brain database. *NeuroImage*, **5**, S425.